



OPEN

Synthesis of no-carrier-added [$^{188, 189, 191}\text{Pt}$]cisplatin from a cyclotron produced $^{188, 189, 191}\text{PtCl}_4^{2-}$ complex

Honoka Obata^{1,2,3}, Katsuyuki Minegishi¹, Kotaro Nagatsu^{1✉}, Mikako Ogawa² & Ming-Rong Zhang¹

We developed a novel method for production of no-carrier-added (n.c.a.) [$^{188, 189, 191}\text{Pt}$]Pt $^{\text{II}}\text{Cl}_4^{2-}$ from an Ir target material, and then synthesized n.c.a. [$^*\text{Pt}$]cis-[Pt $^{\text{II}}\text{Cl}_2(\text{NH}_3)_2$] ([$^*\text{Pt}$]cisplatin) from [$^*\text{Pt}$]Pt $^{\text{II}}\text{Cl}_4^{2-}$. [$^*\text{Pt}$]Pt $^{\text{II}}\text{Cl}_4^{2-}$ was prepared as a synthetic precursor of n.c.a. $^*\text{Pt}$ complex by a combination of resin extraction and anion-exchange chromatography after the selective reduction of Ir $^{\text{IV}}\text{Cl}_6^{2-}$ with ascorbic acid. The ligand-substitution reaction of Cl with NH_3 was promoted by treating n.c.a. [$^*\text{Pt}$]Pt $^{\text{II}}\text{Cl}_4^{2-}$ with excess NH_3 and heating the reaction mixture, and n.c.a. [$^*\text{Pt}$]cisplatin was successfully produced without employing precipitation routes. After this treatment, [$^*\text{Pt}$]cisplatin was isolated through preparative HPLC with a radiochemical purity of 99 + % at the end of synthesis (EOS).

Targeted radionuclide therapy (TRT) is a type of radiation therapy in which malignant tissues are internally irradiated with radiopharmaceuticals emitting with β -ray, α -ray, or Auger electron (Auger e^-). β rays are the most commonly used in the clinic. Recently, α -rays have attracted a great deal of interest because of their high therapeutic efficacy, e.g., ^{225}Ac -PSMA-617 for metastatic castration-resistant prostate cancer¹. Auger e^- , the third candidate, are also expected to be used in TRT, and many radiopharmaceuticals labeled with Auger e^- emitters (e.g., $^{123,125}\text{I}$ and ^{111}In) have been developed². However, the therapeutic efficacy has been modest or low in clinical trials performed to date^{3–7}, and the causes and potential solutions remain unexplored.

An Auger e^- is a low-energy electron released following inner-shell excitation, and each excited atom emits multiple Auger e^- . The range of Auger e^- is extremely short, 2–500 nm, yielding a high linear energy transfer (LET) of 4–26 keV/ μm in the limited nano-scale range⁸. For example, the locally absorbed radiation dose around an ^{125}I decay site was estimated to be 1.6 MGy within a radius of 2 nm⁹. The effective range of Auger e^- is smaller than a single cell, suggesting that it is necessary to transport radiopharmaceuticals to intracellular regions that are sensitive to radiation. DNA is expected to be a prime target of Auger e^- therapy^{2,10–13}. More double-strand breaks can be induced when an Auger e^- emitter is closer to the DNA^{14–16}, suggesting that radiopharmaceuticals must be brought as close as possible to DNA to ensure an efficient interaction between Auger e^- and DNA in the nano-scale range. Therefore, in many radiopharmaceuticals developed to date, Auger-emitting radionuclides of $^{123,125}\text{I}$ and ^{111}In were labeled to DNA-targeting molecules, e.g., a nucleic acid derivative such as deoxyuridine (UdR)^{3,17}, a nuclear localization signal (NLS)^{12,18}, or a DNA-binding molecule^{19–21}, to ensure their transport to DNA. Although antimetabolites based on nucleic acid derivatives are incorporated into DNA, they are limited for use in TRT treatment due to their unavoidable distribution in the intestinal tract, which is radiosensitive. In almost all drugs, however, Auger e^- emitters labeled to DNA-targeting molecules are either not combined with DNA, or are combined indirectly through an intermediary molecule; consequently, there is expected to be a distance between the DNA and the Auger e^- emitter. Auger e^- emitters directly combined with DNA may induce DNA damage most efficiently, but most radioelements are not combined with DNA by themselves. Radioelements should be labeled to intermediary DNA-targeting molecules when being transported to DNA, and such drug design is unalterable.

¹Department of Advanced Nuclear Medicine Sciences, Institute for Quantum Medical Science (iQMS), National Institutes for Quantum and Radiological Science and Technology (QST), 4-9-1 Anagawa, Inage-ku, Chiba 263-8555, Japan. ²Graduate School of Pharmaceutical Sciences, Hokkaido University, Kita-ku, Sapporo, Hokkaido 060-0812, Japan. ³Japan Society for the Promotion of Science (JSPS), 5-3-1 Kojimachi, Chiyoda-ku, Tokyo 102-0083, Japan. ✉email: nagatsu.kotaro@qst.go.jp

	^{195m} Pt	^{193m} Pt	¹⁹¹ Pt	¹⁸⁹ Pt	¹⁸⁸ Pt
Half-life	4.01 d	4.33 d	2.83 d	10.87 h	10.2 d
Decay scheme	IT: 100%	IT: 100%	EC: 100%	EC: 100%	EC: 99+ %
γ	98.9 keV (11.7%)	135.5 keV (0.11%)	538.9 keV (13.7%)	721.4 keV (7.9%)	187.6 keV (19.1%)
Auger e^-	L: 140% K: 3.3%	L: 55.2% K: 0.64%	L: 106% K: 5.3%	L: 108% K: 5.4%	L: 82% K: 3.6%

Table 1. Decay characteristics of relevant platinum radionuclides. Data for ^{188, 189, 193 m, 195m}Pt were taken from NuDat 2.8²³, and data for ¹⁹¹Pt were taken from Radionuclide Decay Data²⁴.

Platinum has a natural property that is useful in this context. Many platinum complexes (e.g., cisplatin, carboplatin, and oxaliplatin) have been used as platinum-based antineoplastic drugs, and platinum complexes with appropriate leaving groups can form direct DNA adducts between Pt and nucleobases²². ¹⁹¹Pt ($T_{1/2}$ = 2.80 d, EC = 100%), ^{193m}Pt ($T_{1/2}$ = 4.33 d, IT = 100%), and ^{195m}Pt ($T_{1/2}$ = 4.01 d, IT = 100%), summarized in Table 1,^{23,24} are promising candidate radionuclides²⁵ that have a suitable half-life and a very high Auger e^- yield, e.g., an average of 32.8 electrons emitted per decay for ^{195m}Pt vs. 14.7 electrons for ¹¹¹In²⁶. Therefore, platinum complexes labeled with radio-Pt as the center metal allow many Auger e^- to be released very close to DNA, and are therefore appropriate for detailed studies to make sure of the degree of the therapeutic effect by Auger e^- . In this work, we focus on cis-[Pt^{II}Cl₂(NH₃)₂] (cis-diamminedichloroplatinum (II)), commonly called cisplatin, which can form direct DNA adducts between Pt and nucleobase as an intra-stand cross-link²². Cisplatin is a widely used chemotherapeutic agent, and its value is supported by a large number of basic and clinical studies over the years. In the clinic, cisplatin is also used in combination with external radiation because it can increase therapeutic efficacy by causing DNA damage via different routes²⁷. Because radio-Pt-labeled cisplatin acts as both an anticancer agent that can target and chemically damage DNA and an Auger e^- emitter, it is expected to provide a superior therapeutic effect as an in vivo radio-chemotherapy agent.

Contrary to these expectations, however, the production method of no-carrier-added (n.c.a.) radio-Pt remains to be established at a practical level. Although the degree of therapeutic efficacy was reported in previous studies using carrier-added radio-cisplatin with low specific activity (~MBq/mg)^{28,29}, it was doubtful whether the fundamental potential of Auger e^- itself could be detected without being masked by the chemotherapeutic effects of non-radioactive cisplatin carriers. To reveal the therapeutic potential of Auger e^- , the DNA-damaging effect of radio-cisplatin needs to be investigated using n.c.a. radio-Pt. Available radio-Pt is commonly produced by a reactor via the ^{nat}Pt(n,x)^{191,193 m, 195m}Pt reaction, resulting in carrier-added radio-Pt derived from a non-radioactive Pt target material. Although n.c.a. ^{191,193m}Pt can be produced by a cyclotron from a target material of iridium (Ir) or osmium (Os), several issues related to the chemical properties of both Ir and Os make it difficult to produce ^{191,193m}Pt with high yield and high purity^{30–33}. Therefore, we demonstrated the production of n.c.a. ¹⁹¹Pt from an Ir target using a cyclotron^{34,35}. In this work, we established a procedure for producing n.c.a. *Pt^{II}Cl₄²⁻ as a synthetic precursor of n.c.a. *Pt complex, as well as a method for synthesis of n.c.a. [*Pt]cisplatin from n.c.a. *Pt^{II}Cl₄²⁻. In the experiments for this study, we used mixed ^{188,189, 191}Pt (81.7 ± 0.4% of ¹⁸⁹Pt, 17.6 ± 0.6% of ¹⁹¹Pt, and 0.7 ± 0.2% of ¹⁸⁸Pt at the end of bombardment [EOB]), described as *Pt in the following, because ^{188,189}Pt is co-produced along with ¹⁹¹Pt from a natural Ir target.

Materials and methods

General. Natural Ir powder (99.9%, d_{50} = 22.560 μ m [median size]) was purchased from Furuya Metal (Tokyo, Japan), and sodium peroxide (95%) was purchased from Hayashi Pure Chemical Industry (Osaka, Japan). Ascorbic acid injection (500 mg/2 mL) was purchased from Fuso Pharmaceutical Industry (Osaka, Japan). Other chemicals and reagents were purchased from FUJIFILM Wako Pure Chemical (Osaka, Japan), Tokyo Chemical Industry (Tokyo, Japan), Kanto Chemical (Tokyo, Japan), Otsuka Pharmaceutical Factory (Tokyo, Japan), or Sigma-Aldrich (St. Louis, MO, USA), and were used in experiments without further purification. Milli-Q ultrapure water was used for dilution in all experiments.

HPGe γ -ray spectrometry was used for radioactivity measurements. The HPGe detector (EGC 15–185-R, Eurisy Measures, Strasbourg, France) was coupled with a 4096 multi-channel analyzer (RZMCA, Laboratory Equipment, Ibaraki, Japan), and calibrated using a mixed (¹⁰⁹Cd, ⁵⁷Co, ¹³⁹Ce, ⁵¹Cr, ⁸⁵Sr, ¹³⁷Cs, ⁵⁴Mn, ⁸⁸Y, and ⁶⁰Co) standard source (Japan Radioisotope Association, Tokyo, Japan). The efficiencies of each chemical separation process were defined as the ratio of ¹⁹¹Pt radioactivity after separation vs. before separation.

The HPLC system (PU-4080i; MD-4010, Jasco, Tokyo, Japan) was equipped with a 200- μ L (analysis) or 1-mL (preparative isolation) sample loop and a radiation detector (US-3000, Universal Giken, Kanagawa, Japan). The analysis of *Pt^{II}Cl₄²⁻ was performed using a Nucleosil SB anionic exchange column (Chemco Plus Scientific, Osaka, Japan) at a flow rate of 1.5 mL/min, and eluted with perchlorate solution (MeCN/H₂O = 40/60 (v/v) containing 0.1 mol/L NaClO₄ and 0.04 mol/L HClO₄). The analysis of [*Pt]cisplatin was performed using a polymer-based aqueous size exclusion chromatography (SEC) column (OHpak SB-804 HQ, Shodex, Showa Denko, Tokyo, Japan) at a flow rate of 1.0 mL/min, eluted with saline solution. Non-radioactive reference samples, K₂Pt^{II}Cl₄ prepared in 0.1 mol/L HCl (0.5 mg/mL), and non-radioactive cisplatin and transplatin in saline solution (0.5 mg/mL) were also analyzed to identify respective retention times.

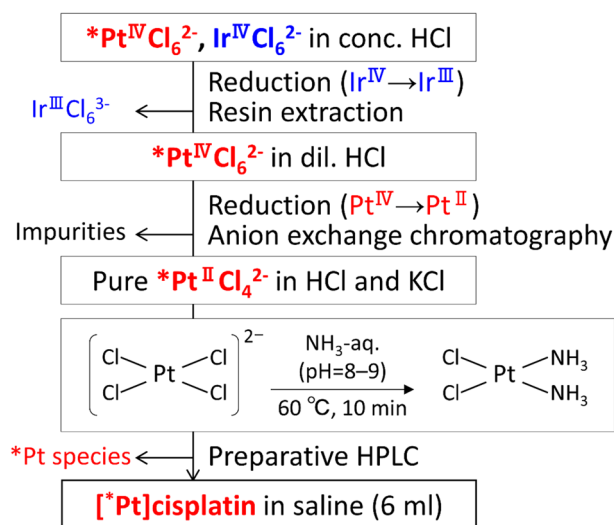


Figure 1. Scheme for preparation of $^{*}\text{Pt}^{\text{II}}\text{Cl}_4^{2-}$ and synthesis of $[^{*}\text{Pt}]\text{cisplatin}$.

Preparation of n.c.a. $^{*}\text{Pt}^{\text{II}}\text{Cl}_4^{2-}$. The preparation scheme is shown in Fig. 1; the details of this scheme are as follows. As described previously^{35, 188,189, 191} Pt was produced via the $^{nat}\text{Ir}(p,xn)^{188,189, 191}\text{Pt}$ reaction with a 30-MeV proton beam for 2–3 h at a beam current of 9–10 μA , and the irradiated Ir target (Ir: 120 mg, Na_2O_2 : 98 mg) was dissolved in 6 mol/L HCl (6 mL). After filtering the solution, a stock solution containing mostly $\text{Ir}^{\text{IV}}\text{Cl}_6^{2-}$ with trace amounts of $^{*}\text{Pt}^{\text{IV}}\text{Cl}_6^{2-}$ was prepared. In a typical batch, about 660 (^{189}Pt) + 142 (^{191}Pt) + 6 (^{188}Pt) MBq of $^{*}\text{Pt}^{\text{IV}}\text{Cl}_6^{2-}$ was produced at EOB ($81.7 \pm 0.4\%$ of ^{189}Pt , $17.6 \pm 0.6\%$ of ^{191}Pt , and $0.7 \pm 0.2\%$ of ^{188}Pt) and was used in the experiments.

Ascorbic acid, a reducing agent, was added to the filtered solution to selectively reduce $\text{Ir}^{\text{IV}}\text{Cl}_6^{2-}$ (ascorbic acid injection/Ir solution = 0.15/6 [v/v]). During this procedure, the dark reddish-brown solution turned greenish-yellow, as $\text{Ir}^{\text{IV}}\text{Cl}_6^{2-}$ was selectively reduced to $\text{Ir}^{\text{III}}\text{Cl}_6^{3-}$ whereas $^{*}\text{Pt}^{\text{IV}}\text{Cl}_6^{2-}$ remained intact. After the reduction, the mixed solution was loaded into a TBP-resin column made by connecting three TBP-resin cartridges (2 mL cartridge, TrisKem International, Rennes, France), as $^{*}\text{Pt}^{\text{IV}}\text{Cl}_6^{2-}$ was selectively extracted into the resin. The column was rinsed with 3 mol/L HCl (5 mL), and then water (6 mL) was used as an eluting agent. To reduce $^{*}\text{Pt}^{\text{IV}}$ to $^{*}\text{Pt}^{\text{II}}$, an ascorbic acid solution (water + ascorbic acid injection = 2 + 8 mL) was added to the collected elution (6 mL), yielding a crude $^{*}\text{Pt}^{\text{II}}\text{Cl}_4^{2-}$ solution. The HCl concentration of this mixed solution was estimated to be < 1 mol/L.

The resultant crude $^{*}\text{Pt}^{\text{II}}\text{Cl}_4^{2-}$ solution (16 mL) was loaded onto a column of QMA ($\Phi 15 \times 40$ mm, AccellPlus QMA, Waters, Milford, MA, USA) for further purification, and the column was rinsed with 0.01 mol/L HCl (12 mL). An aqueous solution containing 1.5 mol/L HCl and 0.02 mol/L KCl, was used as an eluting agent. The elution was fractionated (2 mL each, f1–12), and the fractions containing $^{*}\text{Pt}^{\text{II}}\text{Cl}_4^{2-}$ (f5–10) were collected based on their radioactivity. The volume of the collected solution was decreased by evaporation, and the $^{*}\text{Pt}^{\text{II}}\text{Cl}_4^{2-}$ product (a precursor of $[^{*}\text{Pt}]\text{cisplatin}$) was prepared in HCl and KCl solution (< 300 μL).

Synthesis of n.c.a. $[^{*}\text{Pt}]\text{cisplatin}$. The synthesis scheme is shown in Fig. 1. About 900 μL of 3 mol/L ammonia solution was added to the $^{*}\text{Pt}^{\text{II}}\text{Cl}_4^{2-}$ solution until the pH reached a value of 8–9, as determined using a pH meter (D-72LAB; 9618S-10D, HORIBA, Kyoto, Japan). The mixed solution was heated in hot water at $60\text{ }^{\circ}\text{C}$ for 10 min, and then cooled in ice water. To isolate $[^{*}\text{Pt}]\text{cisplatin}$, preparative HPLC was performed using a polymer-based aqueous size exclusion chromatography (SEC) column (OHPak SB-2004, Shodex, Showa Denko, Tokyo, Japan) at a flow rate of 3.0 mL/min, eluted with physiological saline solution.

Results and discussion

Preparation of n.c.a. $^{*}\text{Pt}^{\text{II}}\text{Cl}_4^{2-}$. We prepared n.c.a. $^{*}\text{Pt}^{\text{II}}\text{Cl}_4^{2-}$ by a combination of resin extraction and anion exchange chromatography as a precursor for the synthesis of n.c.a. $[^{*}\text{Pt}]\text{cisplatin}$. First, $^{*}\text{Pt}^{\text{IV}}\text{Cl}_6^{2-}$ was separated from a bulk Ir target through a TBP-resin column extraction after selectively reducing $\text{Ir}^{\text{IV}}\text{Cl}_6^{2-}$. Our comprehensive survey of reductants revealed that ascorbic acid had the highest selectivity for the reduction of $\text{Ir}^{\text{IV}}\text{Cl}_6^{2-}$ in 6 mol/L HCl. By contrast, $^{*}\text{Pt}^{\text{IV}}\text{Cl}_6^{2-}$ was not reduced at all in 6 mol/L HCl, but was easily reduced in dil. HCl (< 1 mol/L). As a result of the successful selective reduction of $\text{Ir}^{\text{IV}}\text{Cl}_6^{2-}$, only $^{*}\text{Pt}^{\text{IV}}\text{Cl}_6^{2-}$ was extracted from the bulk $\text{Ir}^{\text{III}}\text{Cl}_6^{3-}$ solution onto the extraction column. Ascorbic acid enables the selective reduction of $\text{Ir}^{\text{IV}}\text{Cl}_6^{2-}$ and makes the following separation processes much efficient, compared to acetaldoxime used in our previous study.

In this work, the solid-phase extraction was applied in place of the liquid–liquid extraction because column separation is more suitable for expansion into a remote automatic device for further development. $^{*}\text{Pt}^{\text{IV}}\text{Cl}_6^{2-}$ was extracted onto the TBP-resin column in the presence of HCl, and then quickly eluted with H_2O . The extraction efficiencies for the recovery of $^{*}\text{Pt}$ were above 90% ($n = 3$, Table 2).

	Separation of $^{*}\text{Pt}$ from an Ir target	
	Resin extraction (%)	Purification (AEC) (%)
1	91	61
2	93	60
3	90	70

Table 2. Chemical separation efficiency of $^{*}\text{Pt}$ ($n = 3$). Efficiency contains an uncertainty of 5% in the radioactivity measurement.

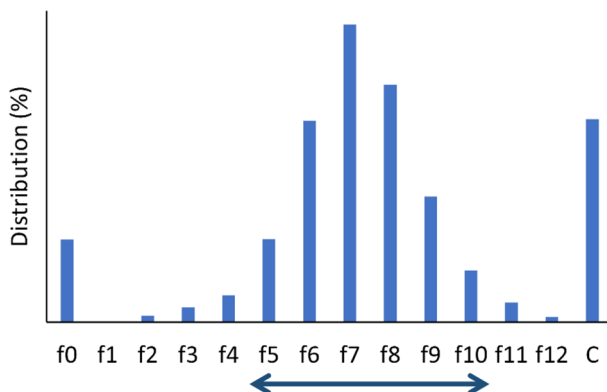


Figure 2. Radiochromatogram obtained during QMA-purification (f0: non-retaining fraction before elution, C: residual on the column). Fractions from f5 to f10 were collected.

While only $\text{Ir}^{\text{IV}}\text{Cl}_6^{2-}$ was reduced by ascorbic acid in 6 mol/L HCl, we found that ascorbic acid is also applicable to reduce $^{*}\text{Pt}^{\text{IV}}\text{Cl}_6^{2-}$ to $^{*}\text{Pt}^{\text{II}}\text{Cl}_4^{2-}$ in dil. HCl (< 1 mol/L). In the reduction of n.c.a. $^{*}\text{Pt}^{\text{IV}}\text{Cl}_6^{2-}$ (< 0.1 nmol), the equivalent amount of reductant is very small, leading to a very low concentration (nmol/L). In that condition, the reducing reaction of n.c.a. $^{*}\text{Pt}^{\text{IV}}\text{Cl}_6^{2-}$ did not proceed by conventional reductants used for $\text{Pt}^{\text{IV}}\text{Cl}_6^{2-}$ underwater (e.g., hydrazine, oxalate, sulfite). Although excess reductants promoted the reduction of n.c.a. $^{*}\text{Pt}^{\text{IV}}\text{Cl}_6^{2-}$ to $^{*}\text{Pt}^{\text{II}}\text{Cl}_4^{2-}$ in a neutralizing solution, undesired hydrolysis or ligand substitution also proceeded and generated unknown species. Therefore, we searched reductants used for n.c.a. $^{*}\text{Pt}^{\text{IV}}\text{Cl}_6^{2-}$ to $^{*}\text{Pt}^{\text{II}}\text{Cl}_4^{2-}$ in HCl, where platinum chloride is more stable, and consequently, ascorbic acid was the most suitable agent in our method for preparing n.c.a. $^{*}\text{Pt}^{\text{II}}\text{Cl}_4^{2-}$.

After elution from the TBP-resin column, $^{*}\text{Pt}^{\text{IV}}\text{Cl}_6^{2-}$ was reduced by ascorbic acid rapidly in < 1 mol/L HCl. Then, the crude $^{*}\text{Pt}^{\text{II}}\text{Cl}_4^{2-}$ solution was purified by anion exchange chromatography (AEC) with a QMA column. The radiochromatogram obtained during QMA-AEC is shown in Fig. 2. Although $^{*}\text{Pt}^{\text{II}}\text{Cl}_4^{2-}$ was predominantly observed (f2–12), some $^{*}\text{Pt}^{\text{II}}\text{Cl}_4^{2-}$ changed to other complexes, which passed through the column without any interaction (f0) or were strongly retained and remained on the column (C), as shown in Fig. 2. Additionally, the early eluted fractions (f1–4) were removed from the product because they contained impurities derived from ascorbic acid. As a result of these losses, a pure fraction of n.c.a. $^{*}\text{Pt}^{\text{II}}\text{Cl}_4^{2-}$ was isolated at an efficiency of 60–70% ($n = 3$, Table 2). Overall, as summarized in Table 2, the efficiency of the preparation of $^{*}\text{Pt}^{\text{II}}\text{Cl}_4^{2-}$ was nearly constant, and the n.c.a. $^{*}\text{Pt}^{\text{II}}\text{Cl}_4^{2-}$ product was obtained. Furthermore, no organic solvents were used in our method for separation of $^{*}\text{Pt}^{\text{IV}}\text{Cl}_6^{2-}$ from a bulk Ir target, which contributes the green chemistry and reduces the workloads on the quality control.

Synthesis of n.c.a. [$^{*}\text{Pt}$]cisplatin. As iodide shows stronger trans effect than chloride, the traditional synthetic scheme of cisplatin involves the conversion of K_2PtCl_4 to K_2PtI_4 ³⁶. Additionally, bulk cisplatin is commonly produced by forming a crystal precipitate^{36,37}. However, it is difficult to precipitate n.c.a. radionuclides (pg-ng), and fewer synthetic steps are suitable to avoid any loss. Therefore, we developed a one-pot radiosynthesis of n.c.a. [$^{*}\text{Pt}$]cisplatin from $^{*}\text{Pt}^{\text{II}}\text{Cl}_4^{2-}$ in solution, and separated it by preparative HPLC. The radiochromatogram obtained during preparative isolation is shown in Fig. 3. [$^{*}\text{Pt}$]cisplatin was detected at a retention time of 28–30 min, in good agreement with the value for non-radioactive cisplatin. The trans isomer (transplatin) was not observed in this radiosynthesis while transplatin is eluted long after cisplatin at 47–49 min (data not shown). The radiochemical yield for [$^{*}\text{Pt}$]cisplatin, defined as the ratio of ^{191}Pt radioactivity of isolated [^{191}Pt]cisplatin to the total ^{191}Pt collected after evaporation, was 5–15%. The low efficiency was due to a decrease in $^{*}\text{Pt}^{\text{II}}\text{Cl}_4^{2-}$ purity during evaporation, in addition to the low synthetic yield of the ligand-substitution reaction between Cl and NH_3 . In HPLC analyses using an anion-exchange column, the peak intensity of $^{*}\text{Pt}^{\text{II}}\text{Cl}_4^{2-}$ decreased with time, whereas an unknown peak that was not retained on the column and a peak of $^{*}\text{Pt}^{\text{IV}}\text{Cl}_6^{2-}$ appeared. The purity of $^{*}\text{Pt}^{\text{II}}\text{Cl}_4^{2-}$ in the evaporated solution was 60% or less, suggesting that n.c.a. $^{*}\text{Pt}^{\text{II}}\text{Cl}_4^{2-}$ is unstable. In support

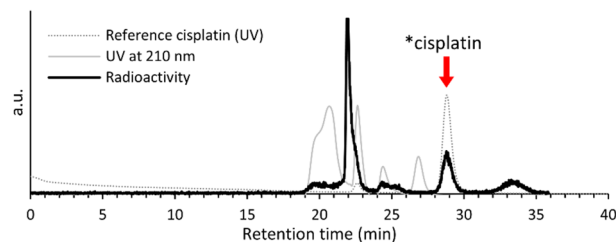


Figure 3. Radiochromatogram obtained during preparative HPLC.

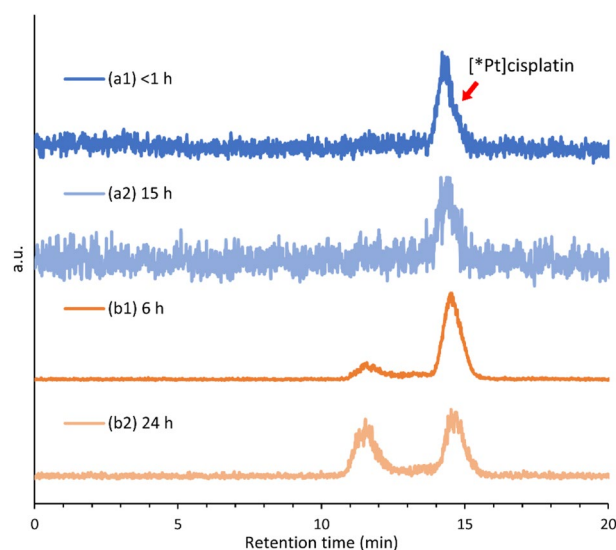


Figure 4. Radiochromatograms of a [*Pt]cisplatin product (a) 0.37 (^{189}Pt) + 0.31 (^{191}Pt) + 0.01 (^{188}Pt) MBq/mL at EOS, (b) 1.76 (^{189}Pt) + 1.40 (^{191}Pt) + 0.05 (^{188}Pt) MBq/mL at EOS.

of this observation, the synthesis yield was increased to 30–40% when the collected elution (1 mol/L HCl and 0.5 mol/L KCl) from the QMA column was used immediately without evaporation.

Even when the purity of $^*\text{Pt}^{\text{II}}\text{Cl}_4^{2-}$ was not so reduced, the synthetic yield was less than 50%. In the conventional synthetic method for bulk cisplatin, the synthetic yield is around 60% when $\text{K}_2[\text{Pt}^{\text{II}}\text{Cl}_4]$ is treated directly with NH_3 , and an accurate two equivalents of NH_3 to Pt should be added in order to prevent excess ligand substitutions^{37,38}. In this study, we used n.c.a. $^*\text{Pt}^{\text{II}}\text{Cl}_4^{2-}$ and treated it with excess NH_3 , probably resulting in low synthetic yield. Nevertheless, it should be noted that heating was essential to promote the ligand substitution reaction between n.c.a. $^*\text{Pt}^{\text{II}}\text{Cl}_4^{2-}$ and excess NH_3 . Without heating, about 50% of $^*\text{Pt}^{\text{II}}\text{Cl}_4^{2-}$ remained unreacted under a pH value of 9, indicating that both NH_3 and heat to some degree promoted ligand substitution for $\sim 10^{-11}$ mol of $^*\text{Pt}$, which was interesting from the standpoint of radiochemistry. Although it is quite difficult to finely control the stoichiometric balance of NH_3 and n.c.a. $^*\text{Pt}^{\text{II}}\text{Cl}_4^{2-}$, an appropriate NH_3 concentration may improve the synthesis yield.

Overall, using our method, n.c.a. [*Pt]cisplatin was finally obtained in saline solution (6 mL) from $^*\text{Pt}^{\text{IV}}\text{Cl}_6^{2-}$ in a bulk Ir target, and at the end of synthesis (EOS), following a one-day cool-down period after EOB, about 1.29 (^{189}Pt) + 1.00 (^{191}Pt) + 0.05 (^{188}Pt) MBq/mL of [*Pt]cisplatin was available for further biological studies.

Quality control. We investigated the radiochemical purity and stability of [*Pt]cisplatin by HPLC analyses. As shown in Fig. 4a1, a single peak of [*Pt]cisplatin was observed with a retention time of 14–15 min. The radiochemical purity of n.c.a. [*Pt]cisplatin was 99% in the final product. Any impurities were below the detection limit in the chromatogram generated by detecting UV absorption at 250 nm. In the sample with low radioactive concentration shown in Fig. 4a1,2 (0.37 (^{189}Pt) + 0.31 (^{191}Pt) + 0.01 (^{188}Pt) MBq/mL at EOS), [*Pt]cisplatin exhibited good stability in the solution, and radiochemical purity was constant up to 15 h after EOS. By contrast, in the high radioactive concentration shown in Fig. 4b1,2 (1.76 (^{189}Pt) + 1.40 (^{191}Pt) + 0.05 (^{188}Pt) MBq/mL at EOS), [*Pt]cisplatin decomposed as time passed. In this higher concentration, the radiochemical purity decreased to 84% (6 h) and 54% (24 h) after EOS. Although reference transplatin was eluted at 22 min, its peak was not observed in all analyses of [*Pt]cisplatin (data not shown). Therefore, the decomposition product at 11–12 min of Fig. 4b1,2 was not transplatin thermodynamically preferred to cisplatin. We assume that [*Pt]

cisplatin decomposed due to hydrolysis or ligand substitution followed by the radiolysis by γ -ray, X-ray, and Auger e^- emitted from ^{191}Pt .

In HPGe γ -ray spectrometry, only $^{188,189,191}\text{Pt}$ were detected, and other coexistent radionuclides in a stock solution (e.g., $^{190}\text{g}, ^{192}\text{g}\text{Ir}$) were below the detection limit after purification with QMA-AEC. Due to the overlapping nuclear reaction channels, the product included not only ^{191}Pt but also $^{188,189}\text{Pt}$ ³⁴.

Conclusions

We developed a novel method for production of $^{191}\text{Pt}^{\text{II}}\text{Cl}_4^{2-}$ from an Ir target by employing the selective reduction of $\text{Ir}^{\text{IV}}\text{Cl}_6^{2-}$ with ascorbic acid. Using a combination of resin extraction and AEC, we prepared n.c.a. $^{191}\text{Pt}^{\text{II}}\text{Cl}_4^{2-}$ as a precursor of [^{191}Pt]cisplatin. N.c.a. [^{191}Pt]cisplatin was successfully obtained by treating n.c.a. $^{191}\text{Pt}^{\text{II}}\text{Cl}_4^{2-}$ with excess NH_3 and heating the reaction mixture. N.c.a. [^{191}Pt]cisplatin was prepared at high radiochemical purities (99 + %), which is useful for evaluating the biological effects of Auger e^- using [^{191}Pt]cisplatin.

Received: 7 December 2020; Accepted: 24 March 2021

Published online: 14 April 2021

References

- Kratochwil, C. *et al.* ^{225}Ac -PSMA-617 for PSMA-targeted α -radiation therapy of metastatic castration-resistant prostate cancer. *J. Nucl. Med.* **57**, 1941–1944 (2016).
- Filosofov, D., Kurakina, E. & Radchenko, V. Potent candidates for Targeted Auger Therapy: Production and radiochemical considerations. *Nucl. Med. Biol.* **94–95**, 1–19 (2021).
- Rebischung, C. *et al.* First human treatment of resistant neoplastic meningitis by intrathecal administration of MTX Plus ^{125}I UdR. *Int. J. Radiat. Biol.* **84**(12), 1123–1129 (2008).
- Vallis, K. A. *et al.* Phase I trial to evaluate the tumor and normal tissue uptake, radiation dosimetry and safety of ^{111}In -DTPA-human epidermal growth factor in patients with metastatic EGFR-positive breast cancer. *Am. J. Nucl. Med. Mol. Imaging* **4**(2), 181–192 (2014).
- Jong, M. *et al.* Somatostatin receptor-targeted radionuclide therapy of tumors: preclinical and clinical findings. *Semin. Nucl. Med.* **32**(2), 133–140 (2002).
- Delpassand, E. S. *et al.* Long-term survival, toxicity profile, and role of F-18 FDG PET/CT scan in patients with progressive neuroendocrine tumors following peptide receptor radionuclide therapy with high activity In-111 pentetreotide. *Theranostics* **2**(5), 472–480 (2012).
- Welt, S. *et al.* Phase I/II study of iodine 125-labeled monoclonal antibody A33 in patients with advanced colon cancer. *J. Clin. Oncol.* **14**, 1787–1797 (1996).
- Kassis, A. I. & Adelstein, S. J. Radiobiologic principles in radionuclide therapy. *J. Nucl. Med.* **46**, 4S–12S (2005).
- Kassis, A. I. *et al.* Radiotoxicity of ^{125}I in mammalian cells. *Radiat Res* **111**, 305–318 (1987).
- Martina, R. F. & Feinendegend, L. E. The quest to exploit the Auger effect in cancer radiotherapy: a reflective review. *Int. J. Radiat. Biol.* **92**(11), 617–632 (2016).
- Buchegger, F., Adamer, F. P., Dupertuis, Y. M. & Delaloye, A. B. Auger radiation targeted into DNA: a therapy perspective. *Eur J Nucl Med Mol Imaging* **33**, 1352–1363 (2006).
- Rosenkranz, A. A., Slastnikova, T. A., Georgiev, G. P., Zalutsky, M. R. & Sobolev, A. S. Delivery systems exploiting natural cell transport processes of macromolecules for intracellular targeting of Auger electron emitters. *Nucl. Med. Biol.* **80**, 45–56 (2020).
- Imstepf, S. *et al.* Nuclear targeting with an auger electron emitter potentiates the action of a widely used antineoplastic drug. *Bioconjugate Chem.* **26**, 2397–2407 (2015).
- Balagurumoorthy, P., Xu, X., Wang, K., Adelstein, S. J. & Kassis, A. I. Effect of distance between decaying ^{125}I and DNA on Auger-electron induced double-strand break yield. *Int. J. Radiat. Biol.* **88**(12), 998–1008 (2012).
- Pereira, E. *et al.* Evaluation of acridine orange derivatives as DNA-targeted radiopharmaceuticals for auger therapy: influence of the radionuclide and distance to DNA. *Sci Rep* **7**, 42544 (2017).
- Reissig, F. *et al.* Direct and auger electron-induced, single and double-strand breaks on plasmid DNA caused by $^{99\text{m}}\text{Tc}$ -labeled pyrene derivatives and the effect of bonding distance. *PLoS ONE* **11**(9), e0161973 (2016).
- Kassis, A. I. *et al.* Intratumoral administration of 5- ^{125}I iodo-2' deoxyuridine in a patient with a brain tumor. *J. Nucl. Med.* **37**, 19S–22S (1966).
- Rosenkranz, A. A. *et al.* Antitumor activity of auger electron emitter ^{111}In delivered by modular nanotransporter for treatment of bladder cancer with EGFR overexpression. *Front. Pharmacol.* **9**, 1331 (2018).
- Yasui, L. S. *et al.* Using hoechst 33342 to target radioactivity to the cell nucleus. *Radiat. Res.* **167**, 167–175 (2007).
- Sato, N. *et al.* Tumor targeting and imaging of intraperitoneal tumors by use of antisense oligo-DNA complexed with dendrimers and/or avidin in mice. *Clin. Cancer Res.* **7**, 3606–3612 (2001).
- Dahmen, V., Pomplun, E. & Kriehuber, R. Iodine-125-labeled DNA-Triplex-forming oligonucleotides reveal increased cyto- and genotoxic effectiveness compared to Phosphorus-32. *Int. J. Radiat. Biol.* **92**(11), 679–685 (2016).
- Johnstone, T. C., Suntharalingam, K. & Lippard, S. J. The next generation of platinum drugs: targeted Pt(II) agents, nanoparticle delivery, and Pt(IV) prodrugs. *Chem Rev* **116**(5), 3436–3486 (2016).
- NuDat 2.8, available online at: <http://www.nndc.bnl.gov/nudat2/index.jsp>.
- Radionuclide Decay Data, available online at: <https://hps.org/publicinformation/radardecaydata.cfm>.
- Qaim, S. M. Nuclear data for production and medical application of radionuclides: present status and future needs. *Nucl. Med. Biol.* **44**, 31–49 (2017).
- Howell RW. Radiation spectra for Auger-electron emitting radionuclides: Report No.2 of AAPM Nuclear Medicine Task Group No.6. *Med Phys* **19**(6):1371–1383.
- Sarraf, M. A. *et al.* Concurrent radiotherapy and chemotherapy with cisplatin in inoperable squamous cell carcinoma of the head and neck. An RTOG study. *Cancer* **59**(2), 259–265 (1987).
- Areberg, J., Wennerberg, J., Johnsson, A., Norrgren, K. & Mattsson, S. Antitumor effect of radioactive cisplatin (^{191}Pt) on nude mice. *Int. J. Rad. Oncol. Biol Phys.* **49**(3), 827–832 (2001).
- Norrgren, K. *et al.* Comparative renal, hepatic, and bone marrow toxicity of cisplatin and radioactive cisplatin (^{191}Pt) in wistar rats. *Cancer Biother. Radiopharm.* **21**(5), 528–534 (2006).
- Parent, M., Strijckmans, K., Cornelis, R., Dewaele, J. & Dams, R. Production of ^{191}Pt radiotracer with high specific activity for the development of preconcentration procedures. *Nucl. Instrum. Methods Phys. Res. Sect. B* **86**, 355–366 (1994).
- Tinker, N. D., Zweit, J., Sharma, H. L., Downey, S. & McAuliffe, C. A. Production of no-carrier added ^{191}Pt , a radiolabel for the synthesis and biological investigations of platinum anti-tumour compounds. *Radiochim. Acta.* **54**, 29–34 (1991).

32. Uddin, M. S. *et al.* Radiochemical determination of cross sections of α -particle induced reactions on ^{192}Os for the production of the therapeutic radionuclide $^{193\text{m}}\text{Pt}$. *Appl. Radiat. Isot.* **68**, 2001–2006 (2010).
33. Uddin, M. S. *et al.* Small scale production of high purity $^{193\text{m}}\text{Pt}$ by the $^{192}\text{Os}(\alpha, 3n)$ -process. *Radiochim Acta* **99**, 131–135 (2011).
34. Obata, H., Khandaker, M. U., Furuta, E., Nagatsu, K. & Zhang, M. R. Excitation functions of proton- and deuteron-induced nuclear reactions on natural iridium for the production of ^{191}Pt . *Appl. Radiat. Isot.* **137**, 250–260 (2018).
35. Obata, H., Minegishi, K., Nagatsu, K., Zhang, M. R. & Shinohara, A. Production of ^{191}Pt from an iridium target by vertical beam irradiation and simultaneous alkali fusion. *Appl. Radiat. Isot.* **149**, 31–37 (2019).
36. Alderden, R. A., Hall, M. D. & Hambley, T. W. The discovery and development of cisplatin. *J. Chem. Educ.* **83**(5), 728 (2006).
37. Kleinberg, J. *Inorganic syntheses*, Vol. 7, 239 (Wiley, 1963).
38. Darensbourg MY. *Inorganic. Syntheses*, Volume 32. New York, Wiley; 1998. 141–144 pp.

Acknowledgements

The authors thank the cyclotron staff for the operation of the NIRS cyclotron AVF-930. We are grateful to Mr. Hisashi Suzuki for technical support and to Dr. Steffen Happel for the sample supply of TBP-resin. This work was supported by JSPS KAKENHI Grant Number JP20J20518.

Author contributions

H.O., K.N., and M.R.Z. wrote the main manuscript. All authors reviewed the manuscript.

Competing interests

The authors declare no competing interests.

Additional information

Correspondence and requests for materials should be addressed to K.N.

Reprints and permissions information is available at www.nature.com/reprints.

Publisher's note Springer Nature remains neutral with regard to jurisdictional claims in published maps and institutional affiliations.



Open Access This article is licensed under a Creative Commons Attribution 4.0 International License, which permits use, sharing, adaptation, distribution and reproduction in any medium or format, as long as you give appropriate credit to the original author(s) and the source, provide a link to the Creative Commons licence, and indicate if changes were made. The images or other third party material in this article are included in the article's Creative Commons licence, unless indicated otherwise in a credit line to the material. If material is not included in the article's Creative Commons licence and your intended use is not permitted by statutory regulation or exceeds the permitted use, you will need to obtain permission directly from the copyright holder. To view a copy of this licence, visit <http://creativecommons.org/licenses/by/4.0/>.

© The Author(s) 2021